NANO LETTERS

2007
Vol. 7, No. 11
3410−3413

# Fabrication of Multiplex Quasi-Three-Dimensional Grids of One-Dimensional Nanostructures via Stepwise Colloidal Lithography

**Gang Zhang,[†] Dayang Wang,* and Helmuth Möhwald**

*Max Planck Institute of Colloids and Interfaces, D-14424, Potsdam, Germany*

*Received July 26, 2007; Revised Manuscript Received September 13, 2007*

**ABSTRACT**

**By using $O_2$-plasma etched monolayers of hexagonally close-packed latex spheres as masks for metal vapor deposition, we successfully demonstrate a stepwise colloidal lithography to stepwise grow highly ordered multiplex quasi-three-dimensional grids of metallic one-dimensional nanostructures, e.g., nanowires and nanorods. The success of the present approach is centered at manipulation of the incidence angle of metal vapor beams with respect to the normal direction of colloidal masks and particularly the azimuth angle $\varphi$ of the projection of the vapor beam incidence on the masks with respect to the vector from one sphere to the nearest neighbors. Stepwise deposition of different metals by regularly varying $\varphi$ allows consecutively stacking of 1D nanostructures into multiplex quasi-3D grids. This stepwise angle-resolved colloidal lithography should provide a significant nanochemical complement of conventional lithographic techniques, enabling us to easily fabricate sophisticated 3D nanostructures with defined vertical and lateral heterogeneity.**

The intensive study of one-dimensional (1D) nanostructures, such as rods, wires, ribbons, and tubes, is driven by their paramount technical applications, for instance being used as interconnects and functional components of nanoscale devices.[1] Up to now, a host of methods to fabricate 1D nanostructures have been successfully established, mainly based on direct crystal growth,[2] seed-mediated crystal growth,[3] anisotropic self-assembly,[4] or template-assisted deposition.[5] The template-assisted process also allows formation of periodic arrays of 1D nanostructures with alignment perpendicular to the supporting substrates. From the point of view of constructing nanoscale devices, however, aligning 1D nanostructures not vertically but horizontally to the substrates is highly demanded.[6] Fabrication of such 1D nanostructure arrays has relied exclusively on lithography, and accessing a higher level of chemical and structural complexity is strongly dependent on the lithography development.

Among the newly developed lithographic techniques, colloidal lithography, using highly ordered interstitial arrays within colloidal crystals as masks or templates to pattern planar and curved surfaces, is of bourgeoning interest due to the process simplicity, the low cost, and the accessibility of scaling down the feature size.[7−16] Nonetheless, colloidal lithography allows only generation of ordered arrays of nanoscale dots. One-dimensional nanostructures and especially their three-dimensional (3D) hierarchical arrays are hard to directly be generated by this means yet. To break this bottleneck, herein we combined plasma-etching of colloidal templates and optimization of the incidence angle of a metal vapor beam and demonstrated a stepwise way of colloidal lithography, which is capable of fabricating quasi-three-dimensional (3D) multiplex grids of metallic nanowires and nanorods.

The monolayers of hexagonally close-packed polystyrene (PS) microspheres were prepared on silicon wafers as masks for metallic vapor deposition via a controlled evaporation process. Prior to the vapor deposition, we conducted two sets of experiments. The first set was to etch the colloidal masks by $O_2$-plasma to convert the close-packed hexagonal arrays of PS spheres into non-close-packed ones. Depending on the sphere diameter, the gap between neighboring spheres was adjusted by the etching period; 20 min etching was sufficient to yield non-close-packed arrays in the case of 830 nm PS spheres. The second set was to determine the sphere packing orientations of hexagonally close-packed PS sphere monolayers using scanning electron microscopy (SEM) to achieve a defined mask registry. Herein we used the azimuth angle ($\varphi$) of the projection of the vapor beam on the masks with respect to the vectors between the nearest-neighboring spheres in the templates to define the mask registry. The

* To whom the correspondence should be addressed. E-mail: dayang.wang@mpikg-golm.mpg.de. Fax: (+49) 331 567 9202.

[†] Present address: State Key Lab of Supramolecular Structures and Materials, College of Chemistry, Jilin University, Changchun 130012, P. R. China.

10.1021/nl071820d CCC: $37.00 © 2007 American Chemical Society
**Published on Web 10/03/2007**

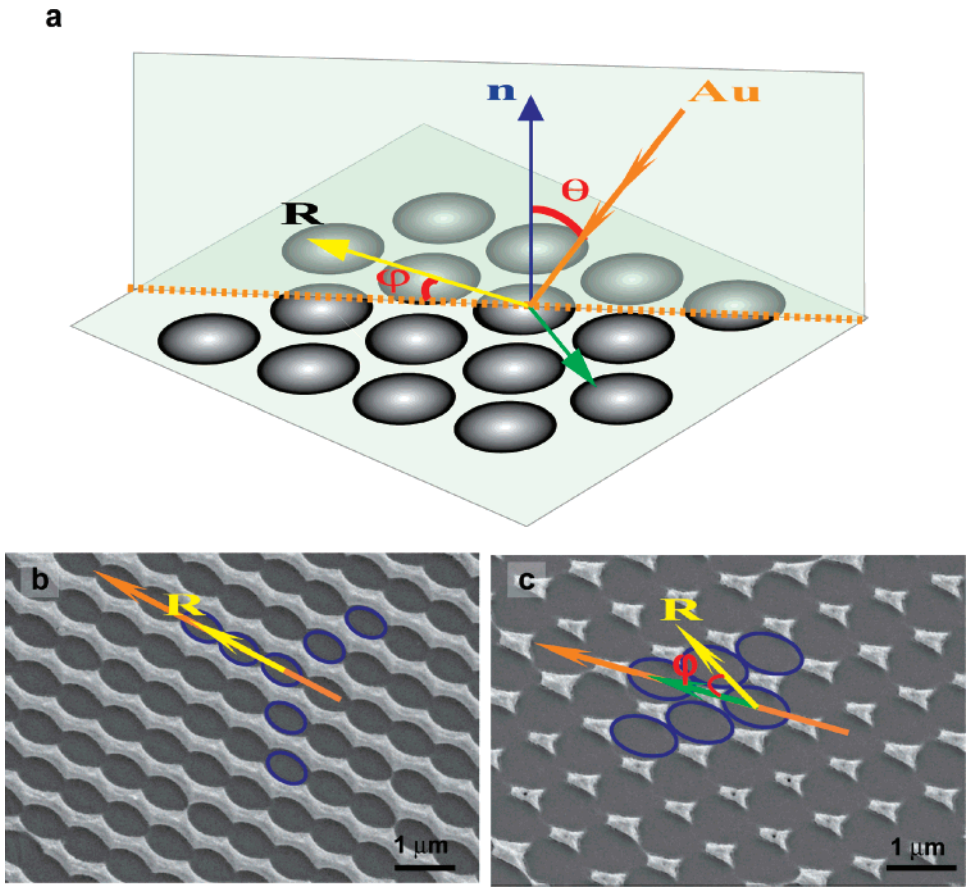


**Figure 1.** (a) Schematic illustration of metallic vapor incidence on a hexagonally non-close-packed sphere monolayer. The vector between nearest-neighbor spheres, the vector between next-nearest-neighbor spheres, and the normal direction of the colloidal template are highlighted by yellow, green, and blue arrows, respectively. The incidence angle ($\theta$) of the vapor beam (orange arrow), with respect to the normal direction of the colloidal masks (blue line), and the azimuthal angle ($\varphi$) of the projection of the vapor beam on the colloidal mask (orange dashed line), with respect to the vector between nearest-neighbor spheres, are marked. One vector (R) between nearest-neighbor spheres is used as the reference. SEM images of 1D nanostructures obtained by using plasma-etched close-packed 830 nm PS sphere monolayers as masks and depositing gold vapor at $\varphi = 0°$ (b) and $\varphi = 30°$(c). The plasma etching time is 20 min, $\theta$ is 45°, and the deposition time is 30 min. The blue circles highlight the original colloidal template spheres.

vectors between the nearest-neighbor spheres and that between the next-nearest-neighbor spheres are marked as yellow and green arrows in Figure 1a, respectively. One vector between the nearest-neighbor spheres, the vector (R), was set as the reference line. Using the resulting non-close-packed monolayers of etched PS spheres as masks for metal vapor deposition led to metal films containing spherical holes hexagonally arranged. By varying the incidence angle ($\theta$) of the metal vapor beam, the angle of the vapor beam with respect to the normal direction of the colloidal masks, from 0° to 15° to 30°, the spherical holes in the metal films were deformed into ellipsoidal ones (Figure S1, Supporting Information). When $\theta$ was increased to 45°, the resulting patterns turned out strongly dependent on the registry of the colloidal masks. When $\varphi = 0°$, that is, the projection of the metal vapor beam on the colloidal mask was co-incident with the vector (R) between the nearest neighbor spheres, zigzag nanowires were obtained and well separated and aligned in parallel (Figure 1b). The width of the resulting zigzag nanowires was dependent on the period of $O_2$-plamsa etching of PS microspheres in a nearly linear fashion (Figure S2 and Table S1, Supporting Information). Despite the decrease of the intervals between the zigzag nanowires obtained, the separation periodicity of their arrays changed little with the etching time, which was well in agreement with the periodicity of the original colloidal templates. On the other hand, when the projection of the metallic vapor beam was co-incident with the vector from next-nearest-neighbor spheres, i.e. $\varphi = 30°$, trapezoidal nanorods were obtained and arranged in a hexagonal array (Figure 1c).

According to the symmetry of a hexagonally non-close-packed sphere monolayer, there are three distinct vectors between nearest-neighbor spheres, marked by yellow arrows in Figure 2a. This encouraged us to conduct stepwise metal vapor deposition by alternating the azimuth angle, $\varphi$, as schematically depicted in Figure 2a. After implementing the first step of metal vapor deposition at $\theta = 45°$ and $\varphi = 0°$ — the project of metal vapor beam on the mask in coincidence with the reference vector (R), we rotated the colloidal mask by 120°, say, the masks were registered at $\varphi = 120°$. Afterward, the second step of metal vapor deposition at $\theta = 45°$ was performed. The removal of the colloidal masks led to the second set of zigzag nanowire arrays on the supporting substrates, crossing the zigzag nanowire arrays

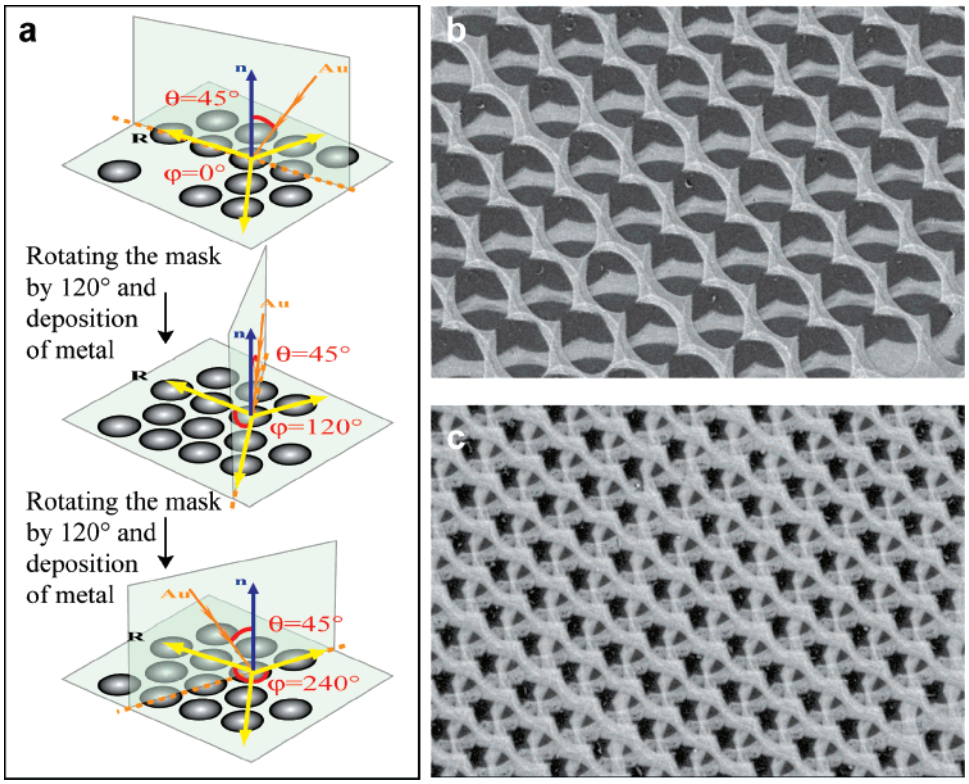


**Figure 2.** (a) Schematic depiction of constructing quasi-3D grids of multiplex zigzang nanowires by stepwise rotating the colloidal mask by 120° with respect to the reference vector (R) between nearest-neighboring spheres over the course of metallic vapor deposition. The projection of metal vapor on the mask was set coincident with the reference vector (R), namely $\varphi = 0°$. SEM images of quasi-3D grids of multiplex zigzag nanowires obtained by stepwise depositing gold, silver, and nickel at $\varphi = 0°$, $\varphi = 120°$, and $\varphi = 240°$ using plasma-etched close-packed 830 nm PS sphere monolayers as masks. The structure obtained by two and three deposition steps are show in (a) and (b), respectively. The plasma etching time is 20 min $\theta$ is 45°, and the deposition time is 30 min.

derived from $\varphi = 0°$ (Figure 2b and Figure S3, Supporting Information). Before removing the colloidal masks, in the current work, we rotated the colloidal masks further by 120° ($\varphi = 240°$) and conducted the third step of metal vapor deposition at $\theta = 45°$. This three-step deposition process yielded three distinct sets of zigzag nanowire arrays fabricated after decomposition of the colloidal templates (Figure 2c). Using atomic force microscopy (AFM) to analyze the height profiles of the resulting structures (Figure S4, Supporting Information), we found that these three distinct sets of zigzag nanowire arrays crossed each other at an angle of 120°; the height of the crossing parts of every two arrays were close to the sum of their thicknesses. SEM imaging of the samples obtained by partially removing the template spheres by using Scotch tape demonstrated the geometric consistency of the resulting grid structures with the three distinct 1D interstitial arrays in line with three vectors between the nearest-neighboring spheres in the colloidal templates (Figure S5, Supporting Information). Thanks to the independence of the chemical nature of the steps in stepwise metal vapor deposition, we chose three different metals for each step: gold for the first step, silver for the second step, and nickel or gold for the third step to the grids shown in Figure 2. Selectively etching or melting of silver nanowires from Au−Ag−Au grids demonstrated their laterally and vertically heterogeneous nature (Figures S6 and S7, Supporting Information). Figures 3 and S8 (Supporting Information) reveal that metal vapor deposition by stepwise and consecutively varying $\varphi$from 30° to 150° to 270° yields new quasi-3D grids composed of trapezoidal nanorods supporting each other and forming a cone with an intersection angle of 120°.

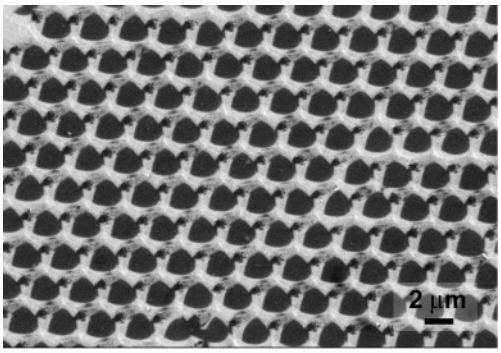


**Figure 3.** SEM image of multiplex quasi-3D grids of multiplex trapezoidal nanorods obtained by stepwise depositing gold, silver, and nickel at $\varphi = 30°$, $\varphi = 150°$, and $\varphi = 270°$ using plasma-etched close-packed 830 nm PS sphere monolayers as masks. The plasma etching time is 20 min $\theta$ is 45°, and the deposition time is 30 min.

Note that the present stepwise angle-resolved colloidal lithography is not limited to the three steps described above. Further stepwise alteration of the azimuth angle as a function of $\varphi = n\cdot120° \text{ or } \varphi = n\cdot120° - 30°$ caused little change of

the structure geometry. Newly formed 1D nanostructure arrays were superimposed on the existing ones but led to 3D woodpile-like grids with a vertical heterogeneity.

In summary, we have successfully fabricated periodic arrays of metallic nanowires and nanorods by using plasma-etched sphere monolayers as masks and adjusting the incidence angle of metal vapor deposition and the registry of the colloidal masks. The incidence angle ($\theta$) of the metal vapor beam and the registry of the colloidal mask, i.e., the azimuth angle ($\varphi$), play a pivotal role for the success of the present methodology. Stepwise variation of $\varphi$ during deposition of metal vapor onto colloidal masks allows different 1D metal nanostructures stacking in quasi-3D and 3D multiplex grids with a defined vertical and especially lateral heterogeneity. Laterally arranging different nanowires into a periodic array with a defined alignment is hard to implement by otherwise means, either conventional lithographic techniques or self-assembly techniques. The present methodology, stepwise angle-resolved colloidal lithography, should provide a significant variant of lithography and pave a facile and elaborate way to construct sophisticated and heterogeneous 3D nanostructures. As a nanochemical complementary tool of conventional lithographic techniques, it therefore holds immense promise in surface patterning. Besides, the resulting multiplex quasi-3D grids should be of significance in technical applications, for instance being used as crossbar switches for microelectronics, as plasmon-assisted enhanced transmission substrates for electro-optics, and stimulation patterned substrates for cell adhesion and growth.

**Acknowledgment.** We thank the Max Planck Society for financial support.

**Supporting Information Available:** The details of experimental method. SEM images of Au films with hexagonally arranged elliptical holes, arrays of zigzag Au nanowires with different widths, multiplex grids composed of zigzag nanowires and those of nanorods, and grids derived from selectively etching and melting of Au nanowires. Tilted SEM images of multiplex grids composed of zigzag nanowires. AFM imaging of multiplex grids composed of zigzag nanowires and those of nanorods.

## References

(1) For a review, see: Xia, Y.; Yang, P.; Sun, Y.; Wu, Y.; Mayers, B.; Gates, B.; Yin, Y.; Kim, F.; Yan, H. *Adv. Mater.* **2003**, *15*, 353.
(2) For a review, see: Scher, E.; Manna, L.; Alivisatos, P. *Phil. Trans. R. Soc. London, Ser. A* **2003**, *361*, 241.
(3) For a review, see: Hu, J.; Odom, T.; Lieber, C. *Acc. Chem. Res.* **1999**, *32*, 435.
(4) For a review, see: Tang, Z.; Kotov, N. *Adv. Mater.* **2005**, *17*, 951.
(5) For a review, see: Hurst, S. J.; Payne, E. K.; Qin, L.; Mirkin, C. *Angew. Chem., Int. Ed.* **2006**, *45*, 2672.
(6) Zhong, Z.; Wang, D.; Cui, Y.; Bockrath, W.; Lieber, C. *Science* **2003**, *302*, 1377.
(7) (a) Hulteen, J.; Treichel, D.; Smith, M.; Duval, M.; Jensen, T.; van Duyne, R. *J. Phys. Chem. B* **1999**, *103*, 3854. (b) Haynes, C.; van Duyne, R. *J. Phys. Chem. B* **2001**, *105*, 5599. (c) Haynes, L.; McFarland, A.; Smith, M.; Hulteen, J.; van Duyne, R. *J. Phys. Chem. B* **2002**, *106*, 1898.
(8) Kosiorek, A.; Kandulski, W.; Glaczynska, H.; Giersig, M. *Small* **2005**, *1*, 439.
(9) Vossen, D. L. J.; Fific, D.; Penninkhof, J.; van Dillen, T.; Polman, A.; van Blaaderen, A. *Nano Lett.* **2005**, *5*, 1175.
(10) von Freymann, G.; John, S.; Kitaev, V.; Ozin, G. A. *Adv. Mater.* **2005**, *17*, 1273.
(11) Choi, D.; Yu, H. K.; Jang, S. G.; Yang, S. M. *J. Am. Chem. Soc.* **2004**, *126*, 7019.
(12) Habenicht, A.; Olapinski, M.; Burmeister, F.; Leiderer, P.; Boneberg, J. *Science* **2005**, *309*, 2043.
(13) McLellan, J.; Geissler, M.; Xia, Y. *J. Am. Soc. Chem.* **2004**, *126*, 10830.
(14) Wang, X.; Lao, C.; Graugnard, E.; Summers, C.; Wang, Z. *Nano Lett.* **2005**, *5*, 1784.
(15) Zhang, G.; Wang, D.; Möhwald, H. *Nano Lett.* **2007**, *7*, 127
(16) Zhang, G.; Wang, D.; Möhwald, H. *Chem. Mater.* **2006**, *18*, 3985.

NL071820D